Journal of Materials Chemistry A

ROYAL SOCIETY OF CHEMISTRY

PAPER

View Article Online
View Journal

Cite this: DOI: 10.1039/d6ta00338a

Mechanochemical synthesis of phase-pure zirconium metal–organic cages

Loris Lombardo, *[ab] Ellan K. Berdichevsky, [c] Farzaneh Fadaei-Tirani, [d] Shin-ichi Orimo, [ae] Andreas Züttel [b] and Satoshi Horike *[fgh]

Zirconium metal–organic cages (Zr-MOCs) exhibit promising applications in adsorption and molecular separation, thanks to their high porosity, stability, and solution processability. However, their synthesis relies on traditional solvothermal methods. In this work, we developed a mechanochemical synthetic route for Zr-MOCs by milling pre-formed Zr-clusters with terephthalic acid. The Zr_3-cluster is easily prepared by combining zirconocene dichloride with carboxylic acids such as acetic acid and benzoic acid. Typical yields of 70% were achieved in only 30 minutes, using a minimal amount of DMF ($\eta = 0.5$ μL g^{-1}). This kinetically controlled strategy produces phase-pure tetrahedral cages with high surface area (>450 m^2 g^{-1}), comparable to those produced by conventional solvothermal processes. The method enables tunable cage architectures by varying ligand identity. The successful synthesis of Zr-MOCs with mono- and bi-functional bidentate ligands, as well as tri-dentate ligands, was achieved, demonstrating the versatility of the mechanochemical approach. This work opens new possibilities for the preparation of Zr-MOCs with insoluble ligands and facilitates scalable production.

Received 13th January 2026
Accepted 1st April 2026

DOI: 10.1039/d6ta00338a

rsc.li/materials-a

Introduction

Porous materials have gained significant attention since the discovery of crystalline molecular framework materials such as covalent organic frameworks (COFs) or metal–organic frameworks (MOFs).[1,2] These materials have been explored for a wide range of applications thanks to their unique structural versatility, with tuneable pore sizes and functionalities.[3] Metal–organic cages (MOCs) represent a new class of discrete, self-assembled structures that combine the design versatility of MOFs with the properties of discrete molecules, such as tunable solubility.[4–6] Among various MOCs, those based on zirconium have attracted significant research interest due to zirconium's remarkable coordination flexibility, strong metal–ligand bonds, and superior chemical stability.[7] These features enable Zr-MOCs to exhibit robust frameworks, making them promising candidates for applications in gas storage and separation, molecular encapsulation, and imaging.[8–11] Yet reproducibly assembling phase-pure, structurally diverse Zr-MOCs remains challenging because conventional solvothermal routes offer limited kinetic control over cluster formation, ligand exchange, and defect generation, leading to non-reproducible results. For example, temperature and solvent decomposition were found to influence the formation and composition of the final cage by the formation of insoluble amorphous solids, such as Zr-clusters.[12] Furthermore, the energy- and solvent-demanding nature of typical solvothermal syntheses conflicts with green-chemistry imperatives and limits scale-up.

Zr-MOCs commonly contain the $[Cp_3Zr_3O(OH)_3(COO)_3]^-$ (Cp = η^5-C_5H_5) secondary building unit (SBU), and can exhibit different cage geometries when built with bidentate ligands, such as tetrahedrons (four SBUs per cage) or "cigars" (two SBUs per cage). Recently, several approaches have been explored to control the geometry and phase-purity of Zr-MOCs. Ligand-based phase control limits the choice of ligands to bulky ones for the formation of pure tetrahedral cages, or rigid, extended ligands for pure "cigar" cages.[13] The type of solvent can also direct the formation of the tetrahedral or "cigar" structure, but it was demonstrated only for selected ligands.[14] The separation of mixtures containing both Zr-MOC geometries has been

[a]Institute for Materials Research, Tohoku University, Sendai, Miyagi 980-8577, Japan. E-mail: lombardo.loris.giovanni.a5@tohoku.ac.jp
[b]Institute of Chemical Sciences and Engineering, Basic Science Faculty, École Polytechnique Fédérale de Lausanne (EPFL) Valais/Wallis, Energypolis, Rue de l'Industrie 17, 1951 Sion, Switzerland
[c]Department of Synthetic Chemistry and Biological Chemistry, Graduate School of Engineering, Kyoto University, Katsura, Nishikyo-ku, Kyoto 615-8510, Japan
[d]Institut des Sciences et Ingénierie Chimiques, École Polytechnique Fédérale de Lausanne (EPFL), 1015 Lausanne, Switzerland
[e]Advanced Institute for Materials Research (WPI-AIMR), Tohoku University, Sendai, Miyagi 980-8577, Japan
[f]Department of Chemistry, Graduate School of Science, Kyoto University, Kitashirakawa-Oiwakecho, Sakyo-ku, Kyoto 606-8502, Japan. E-mail: horike.satoshi.3r@kyoto-u.ac.jp
[g]Institute for Integrated Cell-Material Sciences, Institute for Advanced Study, Kyoto University, Yoshida-Honmachi, Sakyo-ku, Kyoto 606-8501, Japan
[h]Department of Materials Science and Engineering, School of Molecular Science and Engineering, Vidyasirimedhi Institute of Science and Technology, Rayong 21210, Thailand

demonstrated, although the process is laborious and has poor atom economy, requiring large amounts of solvent and AgOTf to solubilize the cages.[15] These limitations underscore the necessity for innovative approaches that allow for the controlled and scalable synthesis of Zr-MOCs with well-defined geometries.

Mechanochemistry has emerged as a powerful green synthetic method for MOFs and other porous materials.[16–22] This technique is environmentally benign (minimal amounts of solvent), allows short reaction times, and is scalable. Mechanochemical synthesis has proven to be effective for preparing phase-pure MOFs by limiting side reactions.[23] It has been extensively studied for the preparation of UiO-type MOFs.[24,25] Most of the reports first prepared the Zr-SBU before milling it with the target ligand.[26–29] In the case of Zr-MOC, the SBU $[Cp_3Zr_3O(OH)_3(COO)_3]^-$ can be prepared using different carboxylic acids such as benzoic acid or acetic acid.[12,30,31] Once the Zr-SBU is ready, ligand substitution in solution was demonstrated as a pathway to get Zr-MOC.[32]

Inspired by the work on UiO MOF synthesis using Zr-SBUs, we report a kinetically guided strategy that combines preformed Zr-cluster with bi-dentate and tri-dentate ligands for the preparation of tetrahedral Zr-cages in only 30 minutes. Mechanochemical synthesis can be conducted with or without DMF and exhibits broad tolerance toward diverse functional groups. Yields exceeding 70% have been achieved, and all resulting cages display high porosity. This synthetic approach may be applicable to insoluble ligands and is ready for scale-up.

Results and discussion

Inspired by the literature, we prepared two easily accessible ZrCp clusters: $[Zr_3(\mu_3\text{-}O)(\mu_2\text{-}OH)_3(Cp)_3(BA)_3]Cl$ (BA = benzoate, $C_7H_5O_2^-$) and $[Zr_3(\mu_3\text{-}O)(\mu_2\text{-}OH)_3(Cp)_3(OAc)_3]Cl$, denoted ZrCp-BA-cluster and ZrCp-OAc-cluster, respectively (Fig. 1). FT-IR and ^1H NMR confirmed the successful synthesis of the two clusters, with only peaks attributed to the ligand, cyclopentadienyl (Cp), and the Zr-cluster present (Fig. S1 and S2). Single crystals (SC) were obtained by re-crystallization in MeOH. The crystal structure of ZrCp-OAc-cluster matches that reported previously.[12] However, the ZrCp-BA-cluster crystal structure has not been reported before. ZrCp-BA-cluster crystallized in the $P\bar{1}$ space group. The structure is composed of trinuclear Zr-clusters with three BA coordinated, as expected. The clusters interact with each other *via* hydrogen bonding and weak interactions, forming a cage-like structure composed of two clusters (Fig. S3).

The crystallographic data is presented in Table S1. Both clusters exhibit thermal stability up to 225 °C and 245 °C for ZrCp-BA-cluster and ZrCp-OAc-cluster, respectively (Fig. S4).

Terephthalic acid (H_2BDC) was selected as the ligand for mechanochemical optimization using ZrCp-OAc-cluster, as the corresponding cage has been reported to form cigar- or tetrahedral-type geometries.[13] Milling was carried out at 500 rpm with DMF as the LAG solvent ($\eta = 0.5$ μL g^{-1}), chosen for its ability to dissolve both precursors and its common use in solvothermal synthesis. Reaction times of 15–60 min were tested with 5 minute pauses every 15 min. The obtained Zr-MOC-BDC powders were washed and activated before measuring N_2 isotherms. Increasing the time from 15 to 30 min improved both yield and surface area of Zr-MOC-BDC, giving >70% yield and a BET surface area of 509 m^2 g^{-1} (Fig. 2A and S5), comparable to phase-pure Zr-BDC-tetrahedral cages prepared solvothermally (462–685 m^2 g^{-1}).[32–34] In contrast, Zr-BDC-cigar cages typically show surface areas <100 m^2 g^{-1}.[13] Mechanochemical synthesis can effectively provide the kinetic product (tetrahedral) thanks to the short reaction time, mild energy input, and low amount of solvent.[35,36] Prolonged milling (60 min) lowered the yield by ~20% and surface area by ~40%. FT-IR spectra confirmed Cp* presence with sharp peaks at ~809 and ~1016 cm^{-1} from the Zr-SBU in all samples (Fig. 2B and S5). However, the 60 min sample displayed a stronger band at 1655 cm^{-1}, consistent with the presence of coordinated DMF.[37] Prolonged milling thus compromises cage integrity through the formation of defects. The rapid ligand exchange between OAc and BDC was confirmed by examining the PXRD patterns after 5

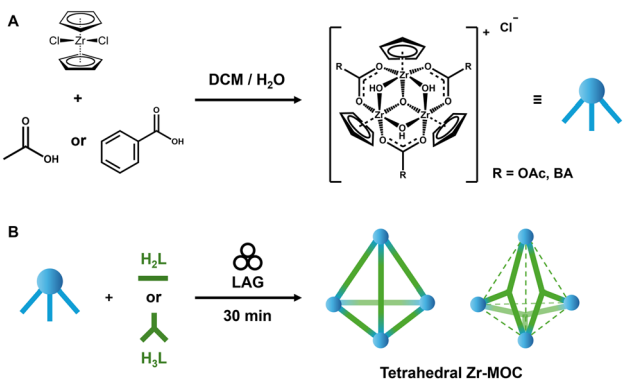

Fig. 1 Schematic representation of the synthesis. (A) Synthesis of Zr-clusters in a bi-phasic solution. (B) Mechanochemical preparation of phase pure zirconium metal organic cage (Zr-MOC) from Zr-cluster and ligands *via* liquid-assisted grinding (LAG).

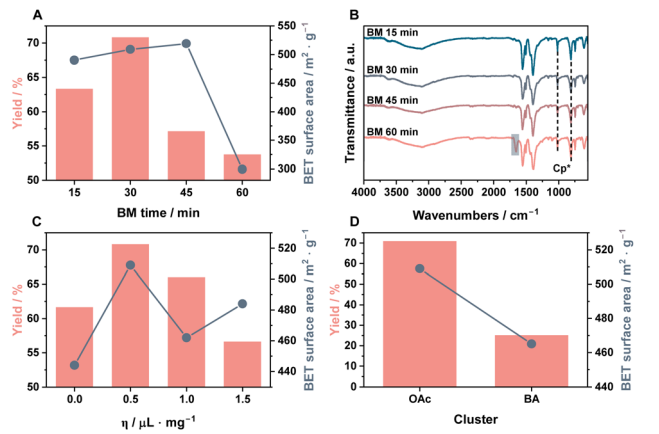

Fig. 2 Optimization of the mechanochemical conditions. (A) The effect of ball-milling time on the yield and BET surface area for Zr-MOC-BDC (DMF $\eta = 0.5$ μL g^{-1}). (B) FT-IR spectra of the prepared Zr-MOC-BDC with different milling times. (C) The effect of DMF amount on the yield and BET surface area of Zr-MOC-BDC (time: 30 min). (D) Comparison of yield and BET surface area of Zr-MOC-BDC prepared with different Zr-clusters (DMF $\eta = 0.5$ μL g^{-1}, 30 min).

minutes of milling (Fig. S6 and S7). While BDC retains its crystalline structure when milled alone, the product becomes weakly crystalline when BDC is milled with ZrCp-OAc, confirming the occurrence of spontaneous ligand exchange. This behavior is readily understood, as the cage is thermodynamically more stable than the cluster.[12,32] In addition, milling the cluster alone can re-arrange the acetate binding from bidentate to monodentate, promoting the exchange with BDC, consistent with the ligand exchange mechanism of Zr_{12} oxo-cluster (Fig. S8).[38] With the milling time fixed at 30 min, DMF content was varied. Across all conditions, the BET surface area remained >450 $m^2\ g^{-1}$ (Fig. 2C and S9). Notably, cage formation under neat grinding is uncommon in ball-milled MOFs, suggesting that acetic acid released during milling may act as an intrinsic LAG agent. The yield increased at $\eta = 0.5\ \mu L\ g^{-1}$ DMF but declined at higher loadings due to slurry formation, which reduces mechanical energy transfer and local heat.[39] The optimized conditions of 30 min milling with $\eta = 0.5\ \mu L\ g^{-1}$ DMF were applied for subsequent screenings.

When ZrCp-BA-cluster was employed instead of ZrCp-OAc-cluster under the optimal conditions, a drastic drop in yield to 25% was observed (Fig. 2D). The surface area and FT-IR of the formed Zr-MOC are consistent with a tetrahedral cage (Fig. S10). We hypothesize two main reasons for the low yield: the release of solid benzoic acid upon milling, which modifies the LAG parameter, and the stronger intermolecular interactions between the ZrCp-BA-clusters, hindering ligand exchange with BDC, as indicated by single-crystal data (Fig. S3). Milling parameters' optimization is certainly possible with ZrCp-BA-cluster, but we focused on ZrCp-OAc-cluster for its higher atom economy. Nuclear magnetic resonance (NMR) and electron-spray ionization mass spectroscopy (ESI-MS) of the optimized Zr-MOC-BDC confirmed the successful preparation of the cage. The ^{1}H NMR displays only 3 main peaks corresponding to the Cp*, ligand, and OH-bridging of Zr-clusters (Fig. S11). ESI-MS peaks at 781.5, 1043.1, and 1564.7 m/z are consistent with $[Zr\text{-}MOC - 4\ Cl^-]^{4+}$, $[Zr\text{-}MOC - 4\ Cl^- - H]^{3+}$, and $[Zr\text{-}MOC - 4\ Cl^- - 2H]^{2+}$ m/z values for the tetrahedron phase (Fig. S12).[33] With the optimized conditions, the mechanochemical synthesis of Zr-MOC-BDC is 16 times faster, and consumes around 7 times less energy and 115 times less solvent (excluding the cluster synthesis), than the conventional solvothermal protocol (Table S2).

To assess the versatility of our newly developed mechanochemical preparation method, we screened various bi-dentate and tri-dentate ligands known to form MOCs by solvothermal synthesis. For the bi-dentate case, 2-amino-terepthalic acid (H_2BDC-NH_2) and 2,6-napthalene dicarboxylic acid (H_2ndc) were selected to examine the influence of functional groups and extended ligand length, respectively. The BM Zr-MOC-BDC-NH_2 and Zr-MOC-ndc exhibit BET surface areas in the same range as previous reports (Fig. 3A and S19, S20).[34,40] Notably, BM Zr-MOC-ndc shows the highest reported surface area (584 $m^2\ g^{-1}$), confirming the phase purity achievable by mechanochemistry.[13,14] The ^{1}H NMR data of both cages are consistent with previous reports, with peaks from the Cp*, Zr-cluster, and ligand (Fig. S14 and S15). FT-IR of Zr-MOC-BDC-NH_2 confirms

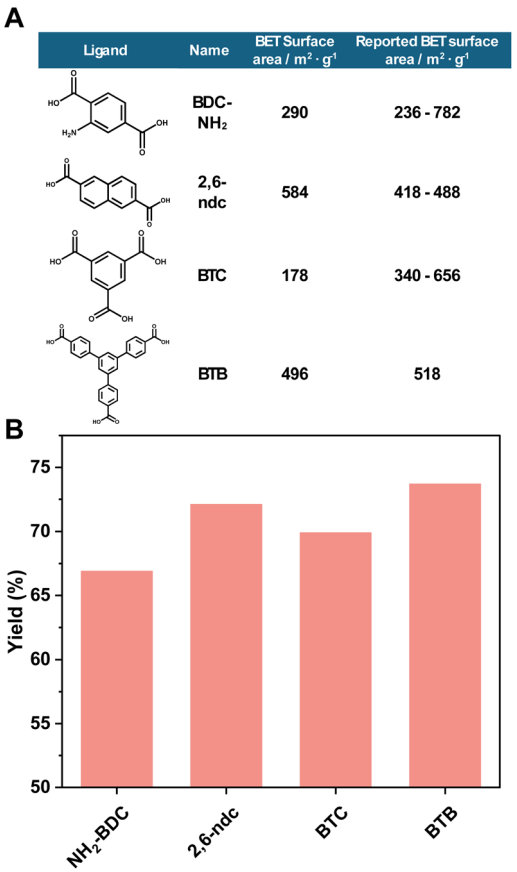

Fig. 3 Versatility of mechanochemical Zr-MOC synthesis. (A) Summary of ligands used and surface area. Reported Zr-cage surface areas: BDC-NH_2,[34,40] 2,6-ndc,[13,14] BTC,[33,41] BTB.[33] (B) Zr-MOC yields from mechanochemical preparation.

the presence of primary amine moieties with a peak around 1335 cm^{-1} (Fig. S13).[40] Moving from bi-dentate to tri-dentate ligands can be challenging due to the higher connectivity, which often leads to defect formation or phase diversity. The mechanochemically prepared cage with trimesic acid (H_3BTC) displays a moderate surface area of 178 $m^2\ g^{-1}$, approximately two times lower than that obtained from solvothermal synthesis (Fig. S18).[33,41] When looking at the ^{1}H NMR spectrum of the cage, we observed multiple peaks for the Cp* and BTC ligand (Fig. S14). The peak splitting of BTC was also observed in solvothermal synthesis and attributed to the presence or absence of DMF inside the cage.[33,41] The pore aperture of Zr-MOC-BTC (4.54 Å) is smaller than the kinetic diameter of DMF (5.95 Å), blocking it from moving out. As mechanochemical synthesis is kinetically controlled in our case (short reaction time and low amount of solvent), the cage cannot rearrange to form guest-free products, which explains the reduced surface area. In the case of Cp*, structural defects could account for variations in the local environment, resulting in multiple signals. Unlike with BDC, milling without solvent didn't produce a porous product, highlighting the challenge of using tri-dentate ligands.

Using the larger 1,3,5-tris(4-carboxyphenyl)benzene (H_3BTB) gave a cage with a surface area close to 500 $m^2\ g^{-1}$, on par with its solvothermal counterpart (Fig. S22).[33] The wider pore width

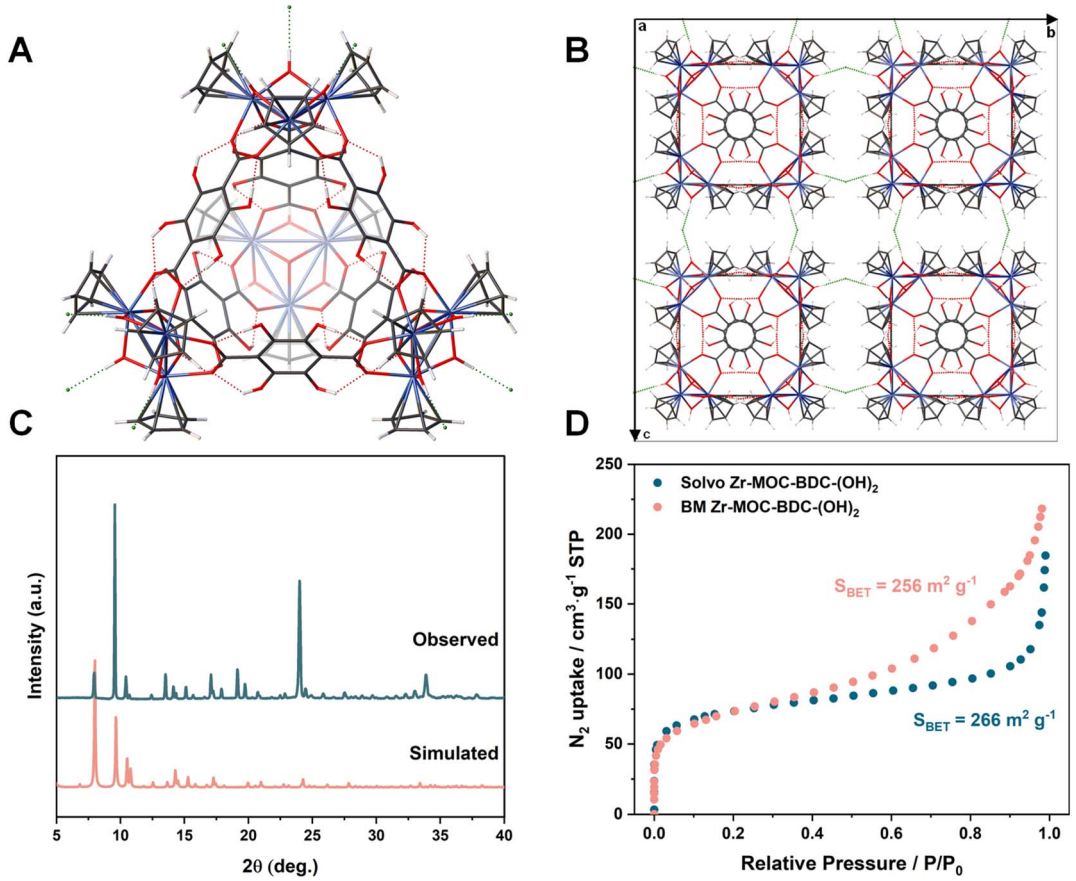

Fig. 4 Solvothermal *versus* mechanochemical synthesis of a new zirconium cage. (A) Crystal structure of Zr-MOC-BDC-$(OH)_2$, and (B) its packing arrangement (white: H, dark grey: C, red: O, blue: Zr, green: Cl). The hydroxyl groups of BDC-$(OH)_2$ are disordered between two configurations. (C) PXRD pattern of the solvothermal Zr-MOC-BDC-$(OH)_2$ compared with the simulated one from single-crystal data. (D) N_2 gas adsorption isotherms at 77 K for Zr-MOC-BDC-$(OH)_2$ prepared by solvothermal or mechanochemical synthesis.

permits the proper activation of Zr-MOC-BTB. ^{1}H NMR spectrum did not show peak splitting of BTB, confirming the formation of a guest-free cage (Fig. S18). However, the Cp* signal has a small peak shoulder, which can originate from the presence of a minor number of defects. The mechanochemical cage formation is promoted by using BTB instead of BTC, thanks to the size of BTB, which avoids steric hindrance between the Zr-clusters.

The tetrahedral geometry of the Zr-MOCs was further confirmed by ESI-MS analysis conducted in MeOH. The expected *m*/*z* peaks corresponding to +4, +3, and +2 tetrahedral ions were observed for Zr-MOC-BDC-NH_2 and Zr-MOC-ndc (Fig. S23 and S24).[13,34] For Zr-MOC-BTC, the main peaks were followed by smaller ones with *m*/*z* differences of approximately 32, 73, and 85, attributed to MeOH, DMF, and DCM molecules trapped within or bound to the cage, respectively (Fig. S25).[33] This is in good agreement with the peak splitting observed by ^{1}H NMR and explains the low surface area. ESI-MS of Zr-MOC-BTB was unsuccessful as it is not soluble in MeOH, but the ^{1}H NMR and FT-IR data support the formation of the cage (Fig. S18 and S26). PXRD patterns of the as-synthesized BM cages show broad signals that partially match the simulated ones obtained from reported single-crystal data (Fig. S27–S30). The MOC crystals are stabilized by weak intermolecular forces among the cages, with solvent molecules playing a crucial role in crystal formation. The activated cages are largely amorphous and exhibit only broad signals, emphasizing their weak intermolecular interactions. The limited amount of DMF combined with the short reaction time likely prevents the development of long-range order, explaining the low crystallinity and deviation from single-crystal data. After washing, only broad signals remain.

As a final proof of concept for our mechanochemical approach, we synthesized a new tetrahedral cage with 2,5-dihydroxyterephthalic acid (BDC-$(OH)_2$) and compared the data with the ball-milled sample. This ligand was selected to test the effect of two functional groups on the mechanochemical synthesis. Yellow cubic crystals were obtained after letting Cp_2ZrCl_2 and BDC-$(OH)_2$ undisturbed in dimethylacetamide for two days, with a yield of around 30%. Single-crystal X-ray diffraction analysis revealed that the new MOC crystallized in the cubic space group $Fm\bar{3}m$, similar to other Zr-MOC structures (Table S3).[34] As expected, Zr-MOC-BDC-$(OH)_2$ is a tetrahedral cage with four $Cp_3Zr_3O(OH)_3$ extremities and six ligands (Fig. 4A). The charge is balanced by chloride anions.

Each cubic unit cell contains eight MOCs interconnected by hydrogen bonds between μ_2-OH of the Zr-SBU and Cl^- (Fig. 4B). The PXRD pattern of the product matched the simulated one (Fig. 4C). The solvothermal cage shows a BET surface area of 266 $m^2\ g^{-1}$, which is lower than Zr-MOC-BDC and Zr-MOC-BDC-NH_2 due to the smaller pore size induced by the hydroxyl groups. Preparing the cage by ball milling with the optimized conditions yields a yellow powder with a PXRD pattern that exhibits broad peaks (Fig. S32). The yield reaches 69% in only 30 min, more than double that of solvothermal synthesis, confirming the advantage of mechanochemistry. The porosity of the ball-milled Zr-MOC-BDC-$(OH)_2$ is almost identical to the solvothermal sample, with a BET surface area of 256 $m^2\ g^{-1}$ (Fig. 4D). The adsorption curve displays a non-well-defined plateau pressure attributed to the small particle size. ^{1}H NMR signals and FT-IR also confirm the successful formation of the mechanochemical cage with signals from the ligand, cluster, and Cp* (Fig. S33 and S34). This demonstrates the functional group tolerance of the mechanochemical synthesis.

Conclusions

We demonstrated for the first time the mechanochemical synthesis of zirconium metal–organic cages by combining preformed Zr_3-clusters with the desired carboxylic acid ligands. The best reaction parameters were determined using BDC as the ligand. A ball-milling time of 30 min with a small DMF amount (η = 0.5 μL g^{-1}) yielded phase-pure tetrahedral cages with a surface area similar to previous reports based on solvothermal reaction. The method proved to be versatile, as Zr-MOCs with functionalized bi-dentate ligands and tri-dentate ligands were successfully prepared. The surface areas are comparable to solvothermal synthesis in almost all cases, demonstrating the effectiveness of mechanochemistry in producing phase-pure products, with the added advantage of higher yields. This new preparation method opens the possibility of synthesizing Zr-MOC containing insoluble ligands or scaling up.

Author contributions

L. L.: conceptualization, data curation, investigation, formal analysis, writing – original draft. E. K. B.: investigation, formal analysis. F. F.-T.: investigation, formal analysis. S. O.: resources, supervision. A. Z.: resources, supervision. S. H.: resources, supervision, and funding acquisition. All authors revised and approved the final version of the manuscript.

Conflicts of interest

There are no conflicts to declare.

Data availability

CCDC 2520154 (ZrCp-BA-cluster) and 2498546 (Zr-MOC-BDC-$(OH)_2$) contain the supplementary crystallographic data for this paper.[42a,b]

The data supporting this article have been included as part of the supplementary information (SI). Supplementary information: Fig. S1–S31, Tables S1, S2, and experimental details. See DOI: https://doi.org/10.1039/d6ta00338a.

Acknowledgements

The work was supported by the Networked Exchange, United Strength for Stronger Partnerships between Japan and ASEAN of Japan Science and Technology Agency (JST-NEXUS, JPMJNX25B4, 2024Y006), Grant-in-Aid for Scientific Research Trans-formative Research Areas (A) "Supra-ceramics" (JP22H05147), fund for the Promotion of Joint International Research (International Collaborative Research, JP24K0112) by the Japan Society of Promotion of Science (JSPS). Loris Lombardo acknowledges the financial support of JSPS Postdoctoral Fellowships for Research in Japan (P21761).

Notes and references

1 C. S. Diercks and O. M. Yaghi, *Science*, 2017, **355**, eaal1585.
2 S. Horike and S. Kitagawa, *Nat. Mater.*, 2022, 1–3.
3 S. Zhang, L. Lombardo, M. Tsujimoto, Z. Fan, E. K. Berdichevsky, Y.-S. Wei, K. Kageyama, Y. Nishiyama and S. Horike, *Angew. Chem., Int. Ed.*, 2023, **62**, e202312095.
4 E.-S. M. El-Sayed and D. Yuan, *Chem. Lett.*, 2020, **49**, 28–53.
5 D. Zhang, T. K. Ronson, Y.-Q. Zou and J. R. Nitschke, *Nat. Rev. Chem.*, 2021, **5**, 168–182.
6 Q.-W. Zeng, L. Hu, Y. Niu, D. Wang, Y. Kang, H. Jia, W.-T. Dou and L. Xu, *Chem. Commun.*, 2024, **60**, 3469–3483.
7 E.-S. M. El-Sayed, Y. D. Yuan, D. Zhao and D. Yuan, *Acc. Chem. Res.*, 2022, **55**, 1546–1560.
8 S. Lee, J. H. Lee, J. C. Kim, S. Lee, S. K. Kwak and W. Choe, *ACS Appl. Mater. Interfaces*, 2018, **10**, 8685–8691.
9 J. Dong, Y. Pan, H. Wang, K. Yang, L. Liu, Z. Qiao, Y. D. Yuan, S. B. Peh, J. Zhang, L. Shi, H. Liang, Y. Han, X. Li, J. Jiang, B. Liu and D. Zhao, *Angew. Chem., Int. Ed.*, 2020, **59**, 10151–10159.
10 W. Fan, S. B. Peh, Z. Zhang, H. Yuan, Z. Yang, Y. Wang, K. Chai, D. Sun and D. Zhao, *Angew. Chem., Int. Ed.*, 2021, **60**, 17338–17343.
11 N. Xu, Y.-X. Tan, E.-S. M. El-Sayed and D. Yuan, *Cryst. Growth Des.*, 2022, **22**, 2768–2773.
12 R. X. Skalla, C. M. Montone, M. Pink, O. K. Walters and E. D. Bloch, *Inorg. Chem.*, 2025, **64**, 6452–6459.
13 A. J. Gosselin, G. E. Decker, B. W. McNichols, J. E. Baumann, G. P. A. Yap, A. Sellinger and E. D. Bloch, *Chem. Mater.*, 2020, **32**, 5872–5878.
14 X. Chen, S.-B. Li, Z.-Y. Liu and Y.-T. Zhang, *J. Solid State Chem.*, 2021, **296**, 121998.
15 B. Le Ouay, M. Tokiwa, R. Ohtani and M. Ohba, *Chem. Mater.*, 2025, **37**, 3414–3422.
16 M. Klimakow, P. Klobes, A. F. Thünemann, K. Rademann and F. Emmerling, *Chem. Mater.*, 2010, **22**, 5216–5221.
17 T. Stolar and K. Užarević, *CrystEngComm*, 2020, **22**, 4511–4525.

18 B. Szczęśniak, S. Borysiuk, J. Choma and M. Jaroniec, *Mater. Horiz.*, 2020, **7**, 1457–1473.
19 Y. Li, W. Chen, G. Xing, D. Jiang and L. Chen, *Chem. Soc. Rev.*, 2020, **49**, 2852–2868.
20 S. Głowniak, B. Szczęśniak, J. Choma and M. Jaroniec, *Mater. Today*, 2021, **46**, 109–124.
21 F. Afshariazar and A. Morsali, *J. Mater. Chem. A*, 2022, **10**(29), 15332–15369.
22 A. Krusenbaum, S. Grätz, G. T. Tigineh, L. Borchardt and J. G. Kim, *Chem. Soc. Rev.*, 2022, **51**(7), 2873–2905.
23 W. D. do Pim, S. Marcotte, A. A. Kitos, P. Richardson, P. Pallister and M. Murugesu, *Inorg. Chem.*, 2022, **61**, 11695–11701.
24 A. M. Fidelli, B. Karadeniz, A. J. Howarth, I. Huskić, L. S. Germann, I. Halasz, M. Etter, S.-Y. Moon, R. E. Dinnebier, V. Stilinović, O. K. Farha, T. Friščić and K. Užarević, *Chem. Commun.*, 2018, **54**, 6999–7002.
25 S. R. Wenger, E. R. Kearns, K. L. Miller and D. M. D'Alessandro, *ACS Appl. Energy Mater.*, 2023, **6**(18), 9074–9083.
26 Y.-H. Huang, W.-S. Lo, Y.-W. Kuo, W.-J. Chen, C.-H. Lin and F.-K. Shieh, *Chem. Commun.*, 2017, **53**, 5818–5821.
27 H. Ali-Moussa, R. Navarro Amador, J. Martinez, F. Lamaty, M. Carboni and X. Bantreil, *Mater. Lett.*, 2017, **197**, 171–174.
28 B. Karadeniz, A. J. Howarth, T. Stolar, T. Islamoglu, I. Dejanović, M. Tireli, M. C. Wasson, S.-Y. Moon, O. K. Farha, T. Friščić and K. Užarević, *ACS Sustain. Chem. Eng.*, 2018, **6**, 15841–15849.
29 L. S. Germann, A. D. Katsenis, I. Huskić, P. A. Julien, K. Užarević, M. Etter, O. K. Farha, T. Friščić and R. E. Dinnebier, *Cryst. Growth Des.*, 2020, **20**, 49–54.
30 J. Li, Z. Gao, L. Han, L. Gao, C. Zhang and W. Tikkanen, *J. Organomet. Chem.*, 2009, **694**, 3444–3451.
31 H. Iden, W. Bi, J.-F. Morin and F.-G. Fontaine, *Inorg. Chem.*, 2014, **53**, 2883–2891.
32 M. G. Sullivan, H. K. Welgama, M. R. Crawley, A. E. Friedman and T. R. Cook, *Chem. Mater.*, 2024, **36**, 567–574.
33 G. Liu, Z. Ju, D. Yuan and M. Hong, *Inorg. Chem.*, 2013, **52**, 13815–13817.
34 L.-Z. Qin, X.-H. Xiong, S.-H. Wang, L.-L. Meng, T.-A. Yan, J. Chen, N.-X. Zhu, D.-H. Liu and Z.-W. Wei, *Inorg. Chem.*, 2021, **60**, 17440–17444.
35 Z. Xiao, H. F. Drake, Y. H. Rezenom, P. Cai and H.-C. Zhou, *Small Struct.*, 2022, **3**, 2100133.
36 M. G. Sullivan, G. E. Sokolow, E. T. Jensen, M. R. Crawley, S. N. MacMillan and T. R. Cook, *Dalton Trans.*, 2023, **52**, 338–346.
37 S. Daliran, A. R. Oveisi, C.-W. Kung, U. Sen, A. Dhakshinamoorthy, C.-H. Chuang, M. Khajeh, M. Erkartal and J. T. Hupp, *Chem. Soc. Rev.*, 2024, **53**, 6244–6294.
38 M. Murali, C. Bijani, J.-C. Daran, E. Manoury and R. Poli, *Chem. Sci.*, 2023, **14**, 8152–8163.
39 L. E. Wenger and T. P. Hanusa, *Chem. Commun.*, 2023, **59**, 14210–14222.
40 D. Nam, J. Huh, J. Lee, J. H. Kwak, H. Y. Jeong, K. Choi and W. Choe, *Chem. Sci.*, 2017, **8**, 7765–7771.
41 Z. Yang, S. B. Peh, S. Xi, Y. Lu, Q. Liu and D. Zhao, *Angew. Chem., Int. Ed.*, 2025, **64**, e202418098.
42 (*a*) CCDC 2520154: Experimental Crystal Structure Determination, 2026, DOI: 10.5517/ccdc.csd.cc2qlf92; (*b*) CCDC 2498546: Experimental Crystal Structure Determination, 2026, DOI: 10.5517/ccdc.csd.cc2pvy8s.